RM No. E8B04

16 JUN 1948

NACA

RESEARCH MEMORANDUM

EFFECT OF AERODYNAMIC HYSTERESIS ON CRITICAL FLUTTER SPEED AT STALL

By Alexander Mendelson

Flight Propulsion Research Laboratory
Cleveland, Ohio

TECHNICAL EDITING WAIVED

NATIONAL ADVISORY COMMITTEE FOR AERONAUTICS

WASHINGTON

June 18, 1948

N A C A LIBRARY
LANGLEY MEMORIAL AERONAUTICAL LABORATORY
Langley Field, Va.

NASA Technical Library
3 1176 01435 5029

NATIONAL ADVISORY COMMITTEE FOR AERONAUTICS

RESEARCH MEMORANDUM

EFFECT OF AERODYNAMIC HYSTERESIS ON CRITICAL FLUTTER SPEED AT STALL

By Alexander Mendelson

SUMMARY

A theoretical analysis was made of the effect of aerodynamic hysteresis on stalling flutter. The assumption was made that the absolute magnitude of the oscillatory aerodynamic forces and moments are the same at stall as at zero angle of attack but that the vector magnitudes of these forces and moments are changed, this change being caused by the lag of aerodynamic damping and restoring forces behind the velocities and displacements at stall, thus giving rise to a hysteresis effect. The decrease of critical flutter speed at stall was thus theoretically shown. The results were applied to a given airfoil and correlation of the experimental and theoretical results was found possible by assuming that the angle of aerodynamic lag varies as the slope of the static-lift curve. The aerodynamic lag was shown to cause the effective torsional damping to decrease thereby explaining the low values of torsional aerodynamic damping obtained at stall.

INTRODUCTION

With the large increase in the use of axial-flow compressors and turbines, an investigation of the vibrations of the blades of these units has become of increasing importance. A significant part of such a study involves the type of vibration that is self-maintained by the continual absorption of energy from the air stream, namely, the flutter of turbine and compressor blades.

The term flutter, as it is ordinarily used, refers to classical flutter, a self-sustained oscillation due to the coupling of inertia forces, elastic forces, damping forces, and dynamic aerodynamic forces. This type of flutter usually occurs on airplane wings at low angles of attack when the velocity reaches a certain value determined by the wing design, and called the critical flutter speed. The theory for this type of flutter has been developed by many investigators and the oscillatory aerodynamic forces and moments derived (references 1 to 3). In all these derivations, the airfoil is assumed to be at zero angle of attack. Close agreement has been found between theory and experiment.

A radically different type of flutter called stalling flutter, however, may occur on profiles at high angles of attack, such as blades near the stall point. This flutter occurs at much lower critical flutter speeds than would be expected from classical-flutter theory. Two reasons exist for believing that this type of flutter would be more likely to occur in compressor and turbine blades than classical flutter: First, compressor and turbine blades are so stiff compared with ordinary airplane wings that critical speeds obtained by classical calculations are usually above the reasonable operating range, at least for subsonic airfoils. This conclusion, however, cannot be stated with certainty because the effect of cascading on the oscillatory aerodynamic forces is as yet unknown. Second, the operation of compressors and turbines at high loads near the stall point makes the occurrence of stalling flutter more likely. Stalling flutter has been shown to occur on compressor cascades in bench tests.

As yet, little is known about the phenomenon of stalling flutter. It has been observed most frequently in connection with stalled propellers (reference 4). Experimental work has shown three possible causes (references 5 to 7). The first cause is termed "static instability" (reference 5) and is associated with the fact that the slope of the lift curve decreases and becomes negative near the stall point. This change of slope can cause an instability, which has been explained by Den Hartog (reference 8) as follows: As the profile moves upward, the resultant motion decreases the effective angle of attack. If the slope of the lift curve is negative, the lift force will increase. As the profile moves downward, the effective angle of attack increases and the lift force decreases. The vibrations therefore continue to build up. This explanation in terms of the static lift curve is, of course, not strictly correct for conditions of flutter because the dynamic-lift curve will be different from the static-lift curve.

The second possible cause for stalling flutter shown to exist (reference 5) was excitation of the airfoil by a system of Kármán vortices shed in the wake. Kármán vortices produce an excitation with frequency directly proportional to the air velocity. At certain discrete velocities, the Kármán vortex frequency will coincide with one of the natural frequencies of the profile. When this coincidence of frequencies occurs, resonant vibrations of the profile can be built up.

The third and apparently most common cause was first investigated by Studer (reference 6) who carried out the first important experimental work on the subject. Studer found that the critical speed of his models dropped considerably near the stall point and that the phase difference between the bending and torsional oscillations decreased to zero so that the torsional and bending motions were in phase. He also found that torsional one-degree-of-freedom flutter was possible, whereas it is known that one-degree-of-freedom classical flutter cannot occur. Studer explained the phenomenon occurring at stall as follows: As the airfoil approaches the stall angle, separation of flow occurs. As the airfoil oscillates about the stall point, the separation of flow is delayed until the position of maximum amplitude is reached. This position will be at an angle of attack greater than that for the stationary airfoil. On the return movement, reestablishment of smooth flow is delayed to an angle of attack below that at which the stationary airfoil would stall. At the stall angle, therefore, the air forces acting depend on the direction of motion, giving rise to a hysteresis loop at stall, as shown in figure 1. Studer came to the conclusion that this hysteresis effect, enabling energy to be absorbed from the air stream, is the cause of stalling flutter.

Studer's work was verified and amplified by Victory (reference 7) who used it as a basis for finding a link between stalling flutter and classical theory. The torsional aerodynamic damping was experimentally shown to decrease as the angle of attack increases and it may become negative at stall. It was then shown that the critical flutter speed at stall could be calculated with reasonable accuracy by classical theory if the usually accepted classical value of the torsional aerodynamic damping is replaced by an experimental value that varies with angle of attack, frequency parameter, Reynolds number, and position of the elastic axis.

A similar hysteresis phenomenon was investigated by Smilg in connection with aileron flutter at transonic speeds. There the flow separation is not due to stall but rather to compressibility effects in the transonic range. The effects, however, are similar. The procedure used was to assume that because of the flow separation the damping and restoring aerodynamic forces and moments lag the velocities and displacements, respectively. This procedure suggested a similar approach to the problem of stalling flutter.

The mathematical theory of the aerodynamic hysteresis effect making use of the concept of an aerodynamic angle of lag developed at the NACA Cleveland laboratory and the results obtained on a given airfoil are presented herein.

914

SYMBOLS

The following symbols are used in this analysis:

a	coordinate of elastic axis measured from midchord, positive towards trailing edge in units of half chord
a_1, b_1, c_1, a_2, b_2, c_2	functions of reduced frequency k and angle of aerodynamic lag φ
a_y, $\overline{a}_y$, a_θ, $\overline{a}_\theta$	aerodynamic coefficients
b	half chord used as reference unit length
b_y, $\overline{b}_y$, b_θ, $\overline{b}_\theta$	aerodynamic coefficients
c	$\mu r_g{}^2$
C_b	stiffness of airfoil in bending per unit span length
C_L	lift coefficient
C_t	stiffness of airfoil in torsion about a per unit span length
e	μr
F	function of reduced frequency k given in reference 1
F_1, F_2	functions of reduced frequency k and angle of aerodynamic lag φ
G	function of reduced frequency k given in reference 1

914

I	moment of inertia about elastic axis per unit span length
i	$\sqrt{-1}$
K	proportionality constant
k	reduced frequency $\frac{\omega b}{v}$
L	oscillatory aerodynamic lift force per unit span
M	oscillatory aerodynamic moment about a per unit span
m	mass of airfoil per unit span
m_a	mass of surrounding air cylinder per unit span, $\pi\rho b^2$
r	location of center of gravity of airfoil measured from a in units of half chord
r_g	radius of gyration referred to a in units of half chord
S	static mass unbalance of airfoil, mrb
t	time
v	critical flutter speed
y	vertical displacement
y_0	maximum bending amplitude
α	static angle of attack
β	phase angle between bending and torsion
θ	angle of torsional displacement
θ_0	maximum torsional amplitude

μ	ratio of mass of profile per unit span to mass of surrounding air cylinder per unit span, $\frac{m}{m_a} = \frac{m}{\pi\rho b^2}$
ρ	density of surrounding air
φ	angle of lag between displacements or velocities and aerodynamic restoring forces or damping forces
ω	frequency of flutter vibration
ω_b	fundamental bending frequency of airfoil
ω_t	fundamental torsional frequency of airfoil

Dots above the symbols represent derivatives with respect to time

914

ANALYSIS

Critical Flutter Speed and Frequency

The oscillatory aerodynamic lift and moment are given by equations XVIII and XX of reference 1. If the exponential relations $y = y_0 e^{i\omega t}$ and $\theta = \theta_0 e^{i(\omega t - \beta)}$ and the relation $k = \frac{\omega b}{V}$ are substituted in these equations in order to eliminate imaginary terms, the equations can be written as follows:

$$\left.\begin{aligned} L &= m_a \left[a_y \ddot{y} - \omega \bar{a}_y y + \left(a_\theta - \frac{1}{k}\bar{a}_y\right) b\ddot{\theta} - \bar{a}_\theta b \dot{\theta} - \omega^2 \frac{\bar{a}_y}{k} b\theta\right] \\ M &= m_a b \left[b_y \ddot{y} - \omega \bar{b}_y y + \left(b_\theta - \frac{1}{k}\bar{b}_y\right) b\ddot{\theta} - \omega \bar{b}_\theta b \dot{\theta} - \omega^2 \frac{\bar{b}_y}{k} b\theta\right] \end{aligned}\right\} \quad (1)$$

where

$$a_y = -\left(1 + \frac{2G}{k}\right)$$

$$\bar{a}_y = \frac{2F}{k}$$

$$a_\theta = a + \frac{2F}{k^2} - \frac{2}{k}\left(\frac{1}{2} - a\right) G$$

$$\bar{a}_\theta = \frac{1}{k} + \frac{2G}{k^2} + \frac{2}{k}\left(\frac{1}{2} - a\right) F$$

$$b_y = a + \frac{2}{k}\left(a + \frac{1}{2}\right) G$$

$$\bar{b}_y = - \frac{2}{k}\left(a + \frac{1}{2}\right) F$$

$$b_\theta = -\left[\frac{1}{8} + a^2 + \frac{2}{k^2}\left(a + \frac{1}{2}\right) F - \frac{2}{k}\left(\frac{1}{4} - a^2\right) G\right]$$

$$\bar{b}_\theta = -\left[\frac{2}{k^2}\left(a + \frac{1}{2}\right) G + \frac{2}{k}\left(\frac{1}{4} - a^2\right) F - \frac{1}{k}\left(\frac{1}{2} - a\right)\right]$$

The second derivative, the first derivative, and the displacement terms in equations (1) represent inertia terms, damping terms, and stiffness terms, respectively. The bending and the torsional displacement are, as has been already indicated, given by

$$y = y_0 e^{i\omega t}$$

and

$$\theta = \theta_0 e^{i(\omega t - \beta)}$$

Equations (1) then become

$$\left.\begin{aligned}
L &= - m_a \, \omega^2 \left[a_y y_0 e^{i\omega t} + i\bar{a}_y y_0 e^{i\omega t} + \left(a_\theta - \frac{\bar{a}_y}{k}\right) b\theta_0 e^{i(\omega t-\beta)} \right. \\
&\quad \left. + i\bar{a}_\theta b\theta_0 e^{i(\omega t-\beta)} + \frac{\bar{a}_y}{k} b\theta_0 e^{i(\omega t-\beta)}\right] \\
M &= - m_a \, \omega^2 b \left[b_y y_0 e^{i\omega t} + i\bar{b}_y y_0 e^{i\omega t} + \left(b_\theta - \frac{\bar{b}_y}{k}\right) b\theta_0 e^{i(\omega t-\beta)} \right. \\
&\quad \left. + i\bar{b}_\theta b\theta_0 e^{i(\omega t-\beta)} + \frac{\bar{b}_y}{k} b\theta_0 e^{i(\omega t-\beta)}\right]
\end{aligned}\right\} \quad (2)$$

These equations represent the vector sum of the aerodynamic inertia, damping, and stiffness forces and moments.

The separation and reestablishment of flow as the airfoil oscillates about the stall point has been shown (reference 6) to lag behind the actual airfoil displacement. The oscillatory aerodynamic forces and moments can be resolved as shown into inertia components in phase with the accelerations, damping components in phase with the velocities, and stiffness components in phase with the displacements. If the flow separation and reestablishment lags the motions, these aerodynamic force and moment components lag the velocities and the displacements. The essential assumption is now made that at stall the absolute values of the oscillating aerodynamic forces and moments are the same as at zero angle of attack but because of the hysteresis effect the vector magnitudes of the aerodynamic restoring forces and moments and the aerodynamic damping forces and moments have so changed that the restoring forces and moments lag the displacements and the damping forces and moments lag the velocities by an angle φ.

Equations (2) are then modified as follows:

$$\left.\begin{aligned}
L &= -m_a\omega^2\left[a_y y_0 e^{i\omega t} + i\bar{a}_y y_0 e^{i(\omega t-\varphi)} + \left(a_\theta - \frac{\bar{a}_y}{k}\right) b\theta_0 e^{i(\omega t-\beta)}\right. \\
&\qquad \left. + i\bar{a}_\theta b\theta_0 e^{i(\omega t-\beta-\varphi)} + \frac{\bar{a}_y}{k} b\theta_0 e^{i(\omega t-\beta-\varphi)}\right] \\
M &= -m_a\omega^2 b\left[b_y y_0 e^{i\omega t} + i\bar{b}_y y_0 e^{i(\omega t-\varphi)} + \left(b_\theta - \frac{\bar{b}_y}{k}\right) b\theta_0 e^{i(\omega t-\beta)}\right. \\
&\qquad \left. + i\bar{b}_\theta b\theta_0 e^{i(\omega t-\beta-\varphi)} + \frac{\bar{b}_y}{k} b\theta_0\, e^{i(\omega t-\beta-\varphi)}\right]
\end{aligned}\right\} \quad (3)$$

The equations of dynamic equilibrium of the system are (reference 1):

$$\left.\begin{aligned}
m\ddot{y} + C_b y + S\ddot{\theta} - L &= 0 \\
S\ddot{y} + I\ddot{\theta} + C_t\theta - M &= 0
\end{aligned}\right\} \quad (4)$$

or

$$\left.\begin{aligned}
&-m\omega^2\, y_0 e^{i\omega t} + C_b y_0 e^{i\omega t} - S\omega^2\, \theta_0 e^{i(\omega t-\beta)} - L = 0 \\
&-S\omega^2\, y_0 e^{i\omega t} - I\omega^2\, \theta_0 e^{i(\omega t-\beta)} + C_t \theta_0 e^{i(\omega t-\beta)} - M = 0
\end{aligned}\right\} \quad (4a)$$

By combining equations (4a) and (3) and dividing the first equation by $m_a\omega^2$ and the second equation by $m_a\omega^2 b$ in order to make the coefficients dimensionless, the following equations are obtained:

$$\left.\begin{aligned}
&\left[\left(a_y - \frac{m}{m_a} + \frac{C_b}{m_a\omega^2}\right) e^{i\omega t} + i\bar{a}_y e^{i(\omega t-\varphi)}\right] y_0 \\
&\quad + \left[\left(a_\theta - \frac{\bar{a}_y}{k} - \frac{S}{m_a b}\right) e^{i(\omega t-\beta)} + \left(\frac{\bar{a}_y}{k} + i\bar{a}_\theta\right) e^{i(\omega t-\beta-\varphi)}\right] b\theta_0 = 0 \\
&\left[\left(b_y - \frac{S}{m_a b}\right) e^{i\omega t} + i\bar{b}_y e^{i(\omega t-\varphi)}\right] y_0 \\
&\quad + \left[\left(b_\theta - \frac{\bar{b}_y}{k} - \frac{I}{m_a b^2} + \frac{C_t}{m_a\omega^2 b^2}\right) e^{i(\omega t-\beta)} \right. \\
&\quad \left. + \left(\frac{\bar{b}_y}{k} + i\bar{b}_\theta\right) e^{i(\omega t-\beta-\varphi)}\right] b\theta_0 = 0
\end{aligned}\right\} \quad (5)$$

Let

$$\frac{m}{m_a} = \mu$$

Then

$$C_b = m\omega_b^{\,2}$$

$$\frac{C_b}{m_a\omega^2} = \mu\, \frac{\omega_b^{\,2}}{\omega^2}$$

$$I = mr_g{}^2b^2; \quad \frac{I}{m_a b^2} = \mu r_g{}^2 = c$$

$$S = mrb$$

$$\frac{S}{m_a b} = \mu r = e$$

$$C_t = I\omega_t{}^2$$

$$\frac{C_t}{m_a\omega^2 b^2} = \mu r_g{}^2 \frac{\omega_t{}^2}{\omega^2} = c\,\frac{\omega_t{}^2}{\omega^2}$$

By substituting into equation (5) and factoring as shown

$$\left.\begin{aligned}
&\left[a_y + \mu\left(\frac{\omega_b{}^2}{\omega^2} - 1\right) + i\bar{a}_y e^{-i\varphi}\right] e^{i\omega t}\, y_0 + \left[\left(a_\theta - \frac{\bar{a}_y}{k} - e\right)\right. \\
&\qquad \left. + \left(\frac{\bar{a}_y}{k} + i\bar{a}_\theta\right) e^{-i\varphi}\right] e^{i(\omega t - \beta)}\, b\theta_0 = 0 \\
&\left[(b_y - e) + i\bar{b}_y\, e^{-i\varphi}\right] e^{i\omega t}\, y_0 + \left[b_\theta - \frac{\bar{b}_y}{k} + c\left(\frac{\omega_t{}^2}{\omega^2} - 1\right)\right. \\
&\qquad \left. + \left(\frac{\bar{b}_y}{k} + i\bar{b}_\theta\right) e^{-i\varphi}\right] e^{i(\omega t - \beta)}\, b\theta_0 = 0
\end{aligned}\right\} \qquad (6)$$

Equations (6) have solutions other than $\theta = y = 0$ if and only if the determinant of the coefficients of y and θ vanishes.

$$\left.\begin{aligned}
&\left[a_y + \mu\left(\frac{\omega_b{}^2}{\omega^2} - 1\right) + i\bar{a}_y e^{-i\varphi}\right] \left[b_\theta - \frac{\bar{b}_y}{k} + c\left(\frac{\omega_t{}^2}{\omega^2} - 1\right)\right. \\
&\qquad \left. + \left(\frac{\bar{b}_y}{k} + i\bar{b}_\theta\right) e^{-i\varphi}\right] - \left[(b_y - e) + i\bar{b}_y\, e^{-i\varphi}\right] \\
&\left[\left(a_\theta - \frac{\bar{a}_y}{k} - e\right) + \left(\frac{\bar{a}_y}{k} + i\bar{a}_\theta\right) e^{-i\varphi}\right] = 0
\end{aligned}\right\} \qquad (7)$$

914

By multiplying through by $e^{i\varphi}$ and substituting the Euler relation

$$e^{i\varphi} = \cos \varphi + i \sin \varphi$$

and by separating real and imaginary parts and rearranging

$$\begin{aligned} a_1 \left(\frac{\omega_t}{\omega}\right)^4 + b_1 \left(\frac{\omega_t}{\omega}\right)^2 + c_1 &= 0 \\ a_2 \left(\frac{\omega_t}{\omega}\right)^4 + b_2 \left(\frac{\omega_t}{\omega}\right)^2 + c_2 &= 0 \end{aligned} \tag{8}$$

where

$$\left.\begin{aligned}
a_1 &= \mu\, c\left(\frac{\omega_b}{\omega_t}\right)^2 (2\cos^2\varphi - 1)\\
a_2 &= \mu\, c\left(\frac{\omega_b}{\omega_t}\right)^2 \sin 2\varphi\\
b_1 &= \left[c(a_y-\mu) + \mu\left(b_\theta - \frac{\overline{b}_y}{k} - c\right)\left(\frac{\omega_b}{\omega_t}\right)^2\right](2\cos^2\varphi - 1)\\
&\quad + \mu\left(\frac{\omega_b}{\omega_t}\right)^2 \frac{\overline{b}_y}{k}\cos\varphi - \left[\mu\left(\frac{\omega_b}{\omega_t}\right)^2 \overline{b}_\theta + c\,\overline{a}_y\right]\sin\varphi\\
b_2 &= \left[c(a_y-\mu) + \mu\left(b_\theta - \frac{\overline{b}_y}{k} - c\right)\left(\frac{\omega_b}{\omega_t}\right)^2\right]\sin 2\varphi\\
&\quad + \mu\left(\frac{\omega_b}{\omega_t}\right)^2 \frac{\overline{b}_y}{k}\sin\varphi + \left[\mu\left(\frac{\omega_b}{\omega_t}\right)^2 \overline{b}_\theta + c\,\overline{a}_y\right]\cos\varphi\\
c_1 &= \left[(a_y-\mu)\left(b_\theta - \frac{\overline{b}_y}{k} - c\right) - \left(a_\theta - \frac{\overline{a}_y}{k} - e\right)(b_y - e)\right](2\cos^2\varphi - 1)\\
&\quad + \left[\overline{a}_\theta(b_y-e) + \overline{b}_y(a_\theta - e) - \overline{b}_\theta(a_y-\mu) - \overline{a}_y(b_\theta - c)\right]\sin\varphi\\
&\quad + \frac{1}{k}\left[\overline{b}_y(a_y-\mu) - \overline{a}_y(b_y-e)\right]\cos\varphi + \overline{b}_y\,\overline{a}_\theta - \overline{a}_y\,\overline{b}_\theta\\
c_2 &= \left[(a_y-\mu)\left(b_\theta - \frac{\overline{b}_y}{k} - c\right) - \left(a_\theta - \frac{\overline{a}_y}{k} - e\right)(b_y - e)\right]\sin 2\varphi\\
&\quad - \left[\overline{a}_\theta(b_y-e) + \overline{b}_y(a_\theta - e) - \overline{b}_\theta(a_y-\mu) - \overline{a}_y(b_\theta - c)\right]\cos\varphi\\
&\quad + \frac{1}{k}\left[\overline{b}_y(a_y-\mu) - \overline{a}_y(b_y-e)\right]\sin\varphi
\end{aligned}\right\} \quad (9)$$

914

914

By solving equation (8) for $\left(\frac{\omega_t}{\omega}\right)^2$ and equating

$$\left(\frac{\omega_t}{\omega}\right)^2 = \frac{-b_1 \pm \sqrt{{b_1}^2 - 4a_1c_1}}{2\,a_1} = \frac{-b_2 \pm \sqrt{{b_2}^2 - 4a_2c_2}}{2\,a_2} \tag{10}$$

or

$$F_1\,(k,\,\varphi) = F_2\,(k,\,\varphi) \tag{11}$$

For a given profile, the functions F_1 and F_2 are functions only of the reduced frequency k and the angle of aerodynamic lag φ. For a given angle of aerodynamic lag φ, equation (11) can be solved for reduced frequency k by finding the intersections of the functions F_1 and F_2 plotted against k. The flutter frequency ω can then be obtained from equation (10) and the critical flutter speed v from the relation

$$v = \frac{\omega b}{k} \tag{12}$$

The critical flutter speeds v and the frequencies k can then be plotted as functions of the angle of aerodynamic lag φ.

Aerodynamic Damping

The torsional aerodynamic damping coefficient $\overline{b}_\theta$ is given by

$$\overline{b}_\theta = \frac{1}{k}\left[\frac{1}{2} - a - 2\left(\frac{1}{4} - a^2\right)F - \frac{2}{k}\left(\frac{1}{2} + a\right)G\right] \tag{13}$$

and is a function of k only. After the reduced frequency k is obtained as a function of the angle of aerodynamic lag φ by equation (11), the torsional aerodynamic damping $\overline{b}_\theta$ can be calculated as a function of the angle of aerodynamic lag φ.

RESULTS AND DISCUSSION

The critical flutter speed v was calculated as a function of the angle of aerodynamic lag φ by means of equations (11) and (12) for wing II of reference 7. The constants for this wing are:

$$a = -0.29$$

$$b = 3.375 \text{ inches}$$

$$r = 0.228$$

$$\mu = 161.2$$

914

$$\omega_t = 87.2 \text{ radians per second}$$

$$\omega_b = 80.3 \text{ radians per second}$$

The radius of gyration r_g, which was not given, was assumed to equal 0.5. The results are shown in figure 2. As the angle of aerodynamic lag φ increases, the critical flutter speed $\overline{v}$ decreases. If the torsional aerodynamic damping coefficient $\overline{b}_\theta$ is now calculated by means of equation (13), the curve shown in figure 3 is obtained. The torsional aerodynamic damping coefficient $\overline{b}_\theta$ decreases with increasing angle of lag φ. From figures 2 and 3 the critical flutter speed $\overline{v}$ can be obtained as a function of the torsional damping coefficient $\overline{b}_\theta$. This relation is plotted in figure 4 and shows the critical flutter speed $\overline{v}$ decreasing as the torsional damping $\overline{b}_\theta$ decreases. The shape of this curve is very similar to those obtained in reference 7 for ratios of torsional to bending frequency ω_t/ω_b close to 1.

The results obtained thus far indicate that the aerodynamic-lag effect can account for a drop in critical flutter speed $\overline{v}$ in the region of stall and also for a decrease in torsional aerodynamic damping. In order to obtain quantitative agreement with the experimentally observed critical flutter speeds in the region of stall, however, it is necessary to find a relation between the angle of aerodynamic lag φ and the angle of attack α. Figure 7 of reference 5 shows the variation of critical flutter speed $\overline{v}$ with angle of attack α for this airfoil. By cross-plotting this curve with figure 2, the angle of aerodynamic lag φ can be obtained as a function of angle of attack α. This relation is shown plotted as a solid line in figure 5.

The question now presents itself of whether some physical basis can be found for the curve shown in figure 5. A relation between angle of attack α and the angle of aerodynamic lag φ suggests itself when the lift curve of the airfoil is considered. As the angle of attack α increases, the separation of flow increases and the slope of the lift curve decreases. Also, as the separation of flow increases, the angle of aerodynamic lag φ might be expected to increase. It would therefore seem possible that the angle of aerodynamic lag φ is related to the change of slope of the lift curve. The lift curve for the airfoil used is given in reference 5. The assumption was now made that the angle of aerodynamic lag φ is given by

$$\varphi = K\left[\left(\frac{dC_L}{d\alpha}\right)_{\alpha=\alpha_0} - \frac{dC_L}{d\alpha}\right]$$

The slope of the lift curve at zero angle of attack is approximately 2π and the constant K was calculated by taking one arbitrary point from the solid curve of figure 5. The value of K is equal to $45/\pi$ if the angle of aerodynamic lag φ is in degrees. Therefore,

$$\varphi = \frac{45}{\pi}\left(2\pi - \frac{dC_L}{d\alpha}\right) \qquad \varphi_{radians} = \frac{1}{4}\left(2\pi - \frac{dC_L}{d\alpha}\right) \tag{14}$$

This equation was plotted as the dashed curve of figure 5 and is seen to agree very well with the solid curve, which is based on experimental data.

By combining the dashed curve of figure 5 with the relation shown in figure 2, the critical flutter speed v can now be plotted as a function of angle of attack α. This function is shown as the dashed curve of figure 6, which agrees very well with the experimental curve obtained from figure 7 of reference 5. (The slope of the lift curve shown in reference 5 by means of which the dashed curve of fig. 5 was obtained is plotted in fig. 7 of this report.)

The torsional aerodynamic damping $\bar{b}_\theta$ can now also be plotted as a function of the angle of attack α (fig. 8). The torsional aerodynamic damping $\bar{b}_\theta$ drops sharply in the region of stall, the shape of the curve being similar to the shape of the critical flutter-speed curve shown in figure 6.

SUMMARY OF RESULTS

From the calculations of critical flutter speeds made for a given airfoil, it was shown that the phenomenon of stalling flutter can at least in some cases be explained on the basis of an aerodynamic lag or hysteresis effect. The general characteristics of stalling flutter, namely, decreases in critical flutter speed and in effective aerodynamic torsional damping coefficient with increasing angle of attack, were shown to be related to the more fundamental concept of lagging aerodynamic forces and moments. Correlation between experimental and theoretical results was obtained by assuming that the aerodynamic angle of lag varies with the angle of attack in a manner that can be explained by the variation in the slope of the static-lift curve. More experimental and theoretical work is necessary to more closely correlate the aerodynamic lag with the angle of attack. 914

Flight Propulsion Research Laboratory,
National Advisory Committee for Aeronautics,
Cleveland, Ohio.

REFERENCES

1. Theodorsen, Theodore: General Theory of Aerodynamic Instability and the Mechanism of Flutter. NACA Rep. No. 496, 1934.

2. Duncan, W. J., and Collar, A. R.: Calculation of the Resistance Derivatives of Flutter Theory. I. R. & M. No. 1500, 1932.

3. Kassner, R., and Fingado, H.: The Two-Dimensional Problem of Wing Vibration. R.A.S. Jour., vol. XLI, Oct. 1937, pp. 921-944.

4. Sterne, L. H. G., and Ewing, H. G.: A Comparison of Flutter Tests on Propellers with 2, 3, and 4 Blades. Rep. No. S.M.E. 3287, R.A.E., 1944.

5. Bollay, William, and Brown, Charles D.: Some Experimental Results on Wing Flutter. Jour. Aero. Sci., vol. 8, no. 8, June 1941, pp. 313-318.

6. Studer, H.: Experimental Study of Wing Flutter. A.R.C. Oscil. Paper No. 60.

7. Victory, Mary: Flutter at High Incidence. Rep. No. S.M.E. 3240, R.A.E., 1943.

8. Den Hartog, J. P.: Mechanical Vibrations. McGraw-Hill Book Co., Inc., 2d ed., 1940, p. 343.

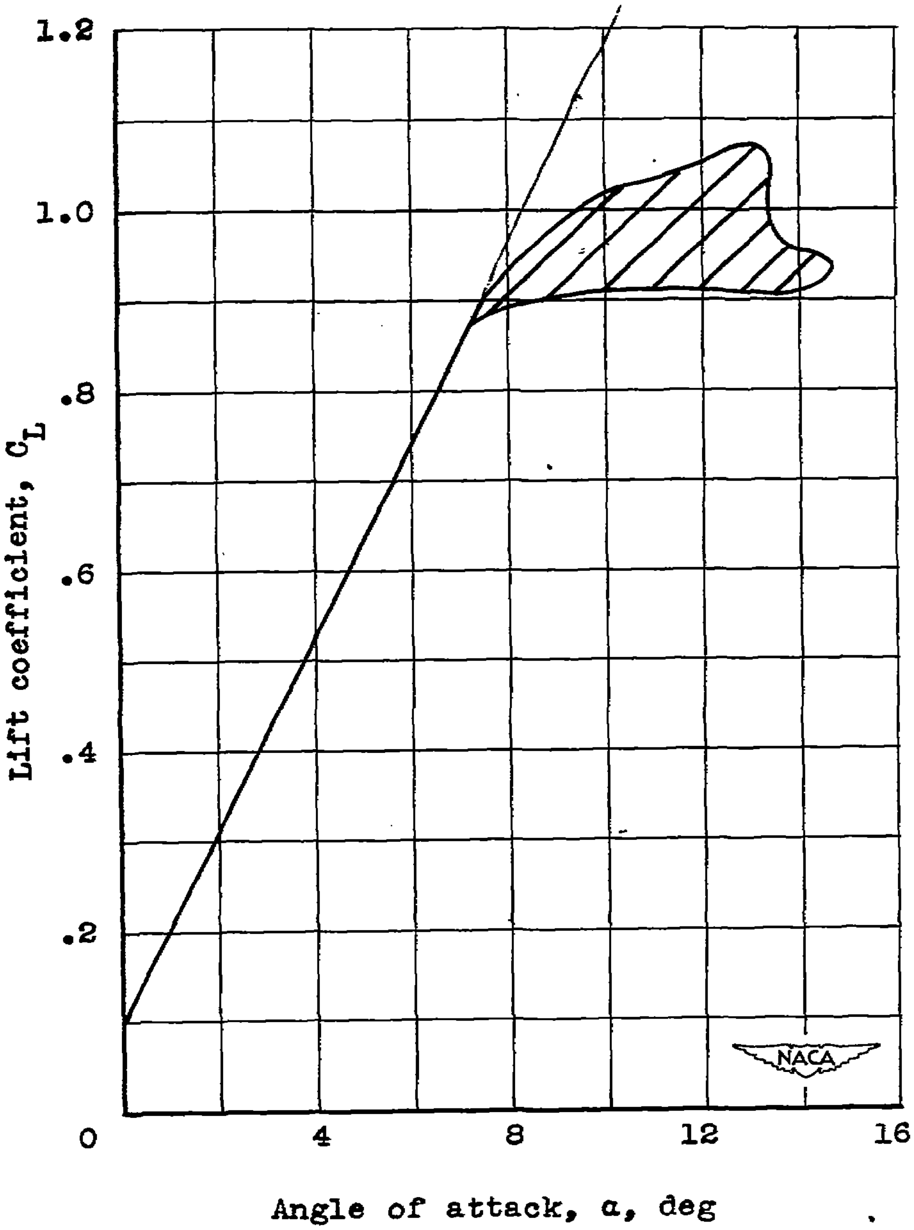

Figure 1. - Typical lift curve showing hysteresis loop.

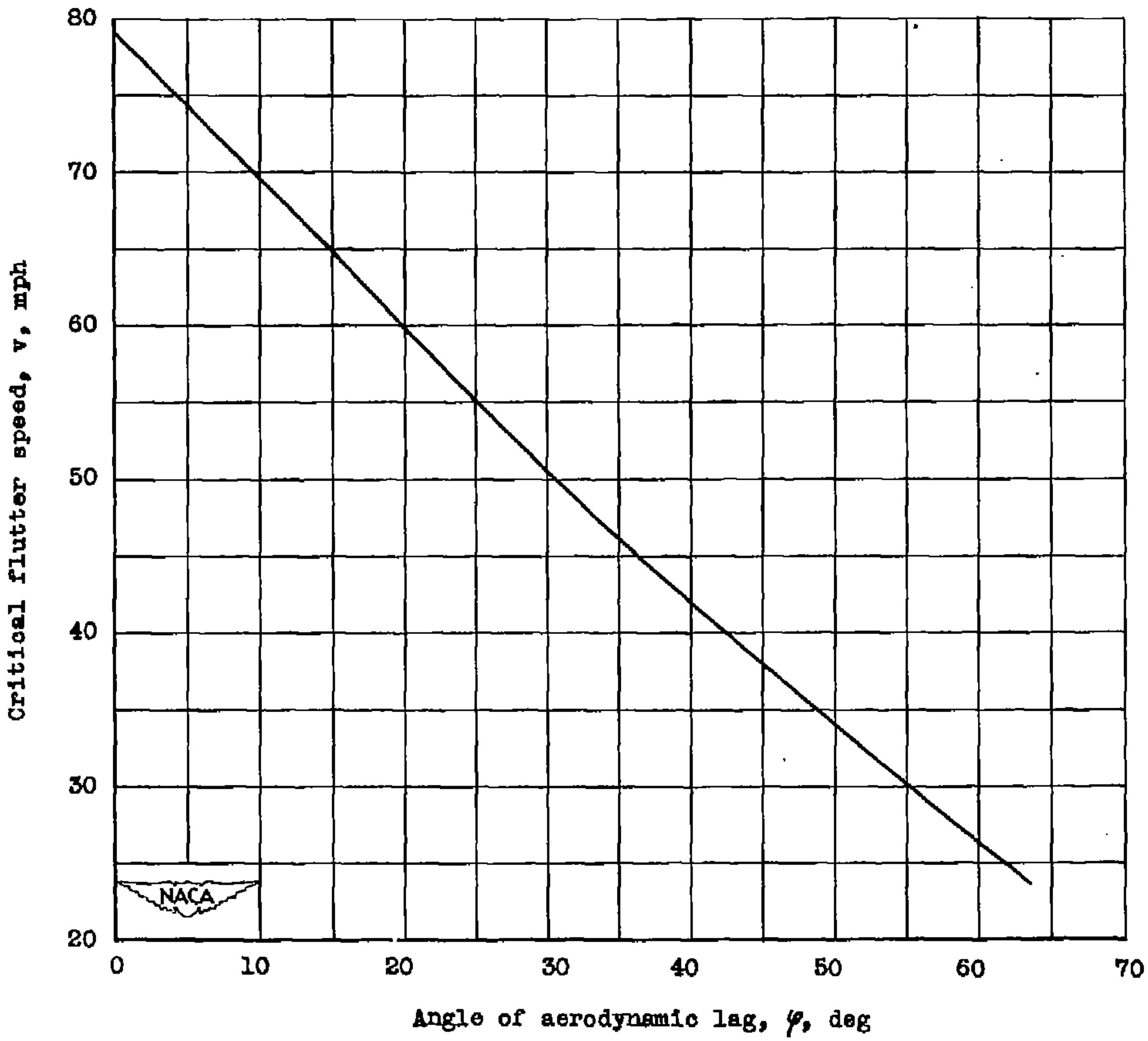

Figure 2. - Variation of theoretical critical flutter speed with angle of aerodynamic lag.

914

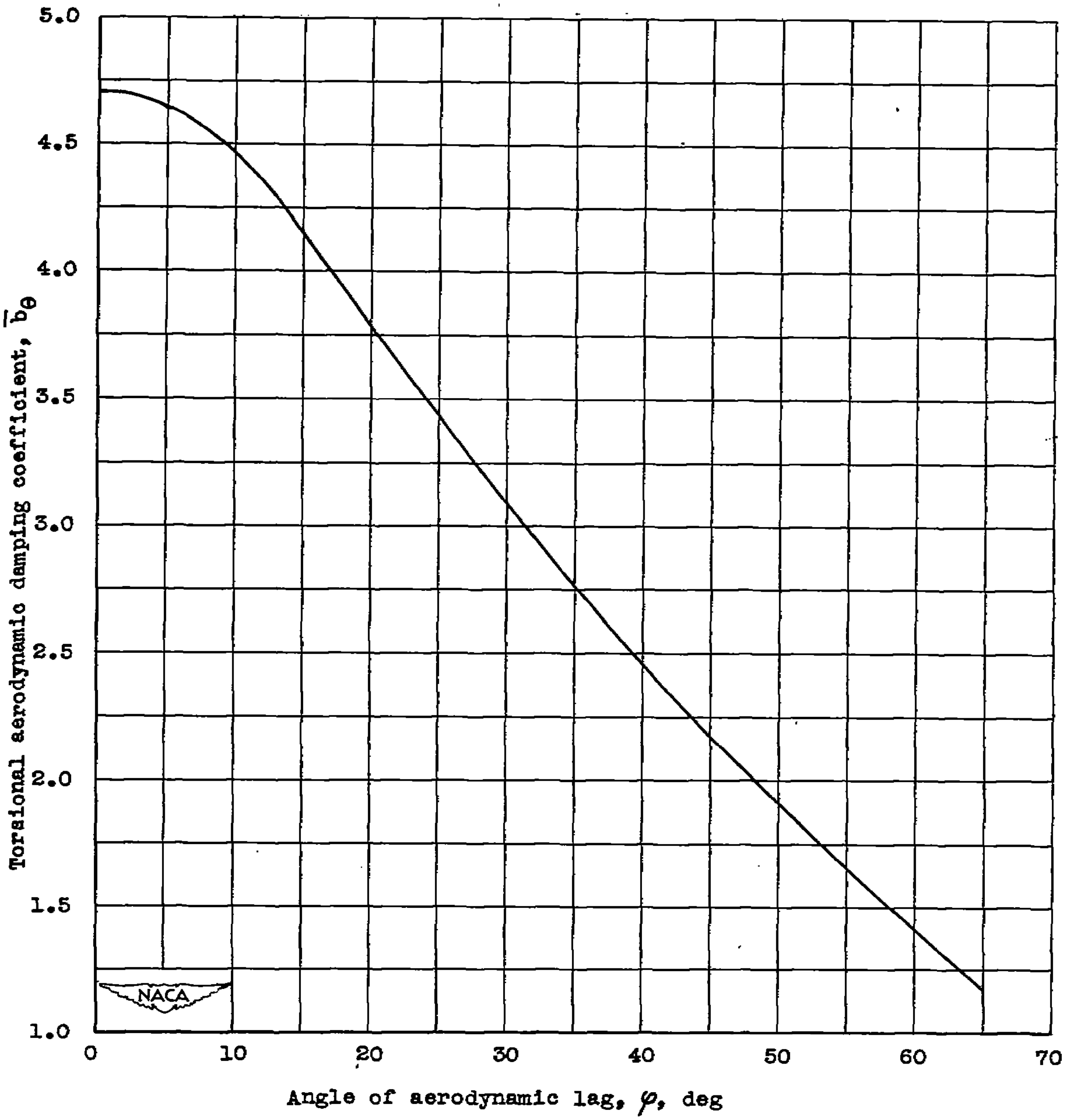

Figure 3. - Variation of theoretical torsional aerodynamic damping coefficient with angle of aerodynamic lag.

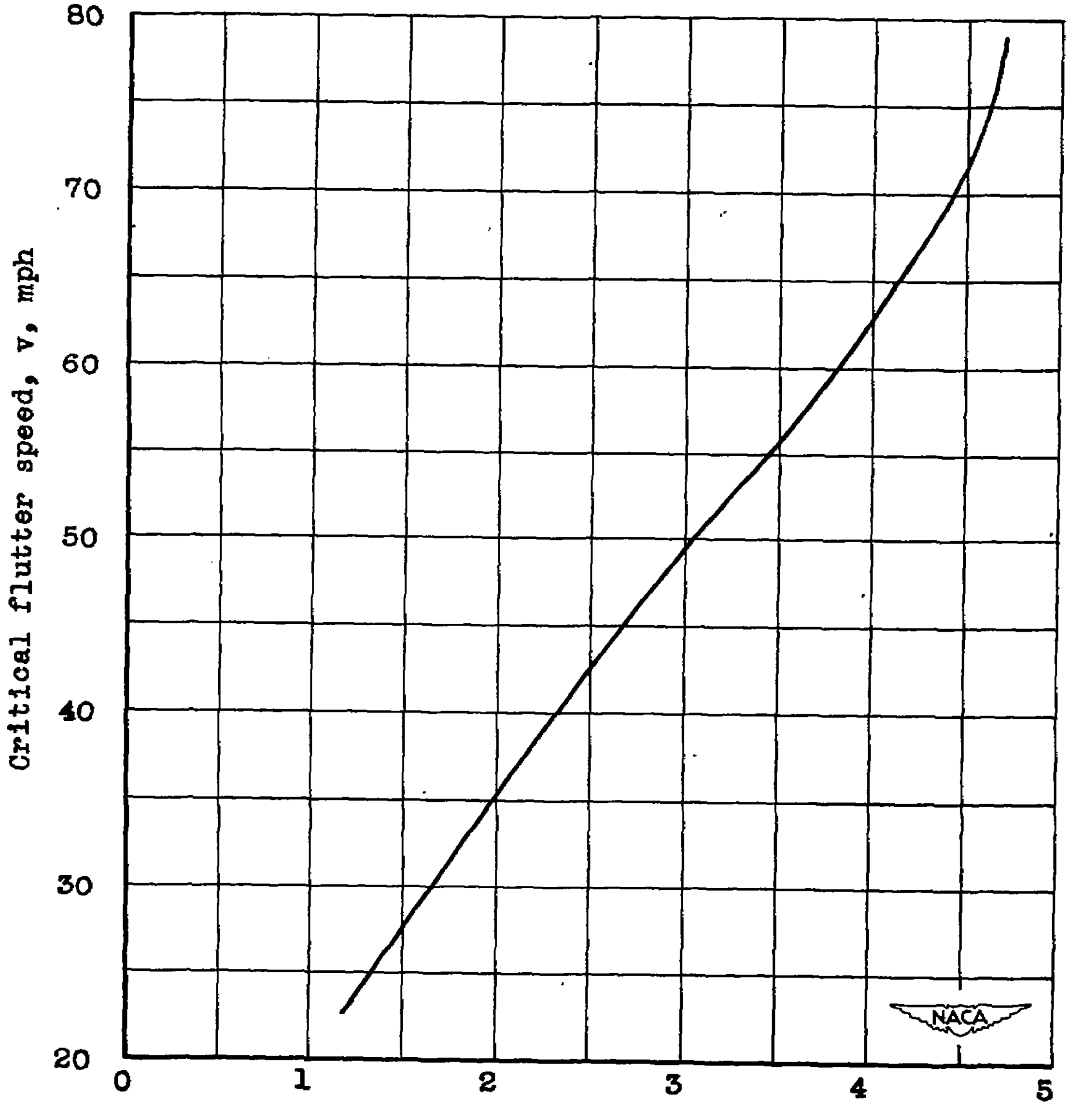

Figure 4. - Variation of theoretical critical flutter speed with torsional aerodynamic damping coefficient.

914

914

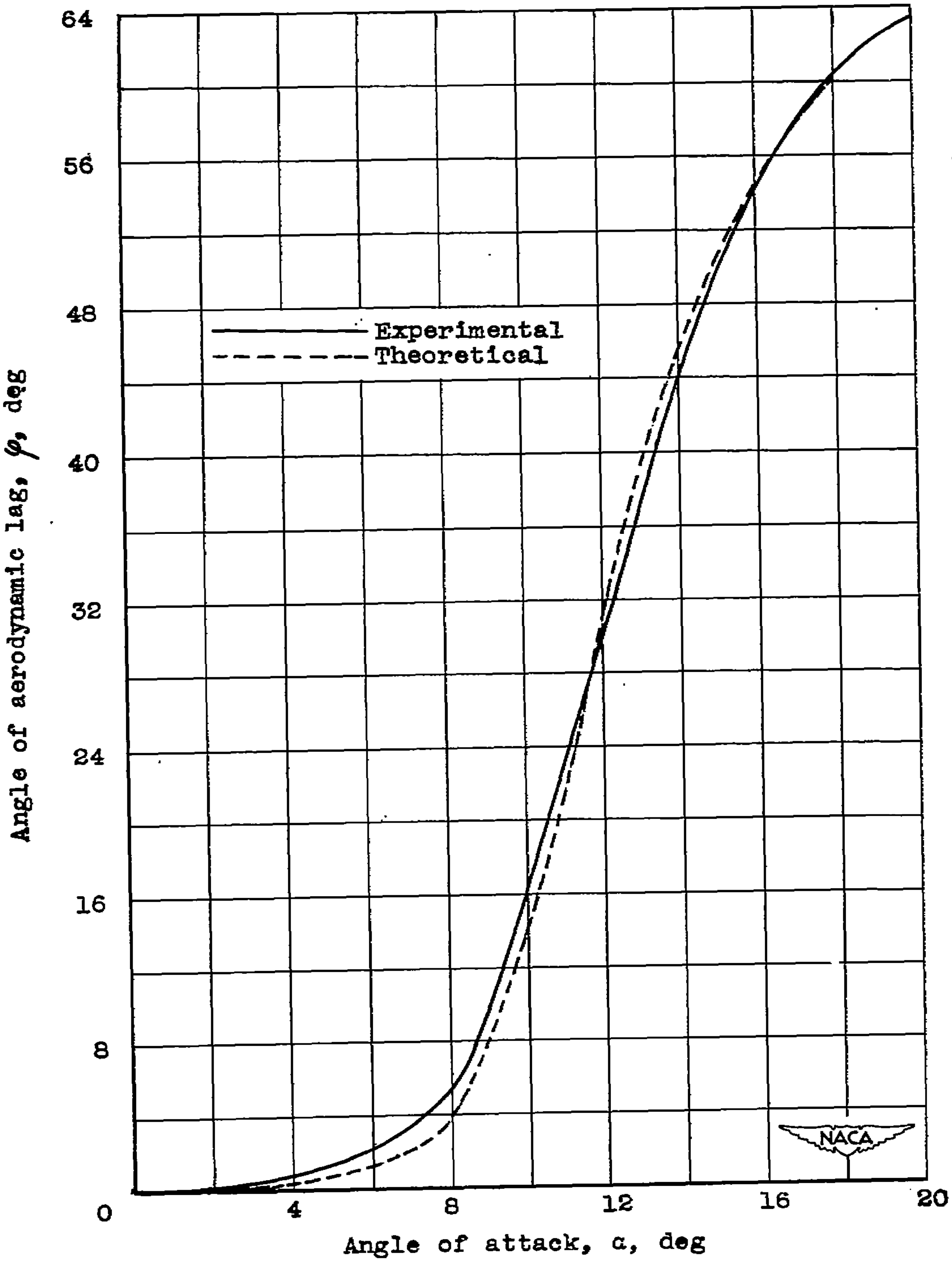

Figure 5. - Variation of angle of aerodynamic lag with angle of attack.

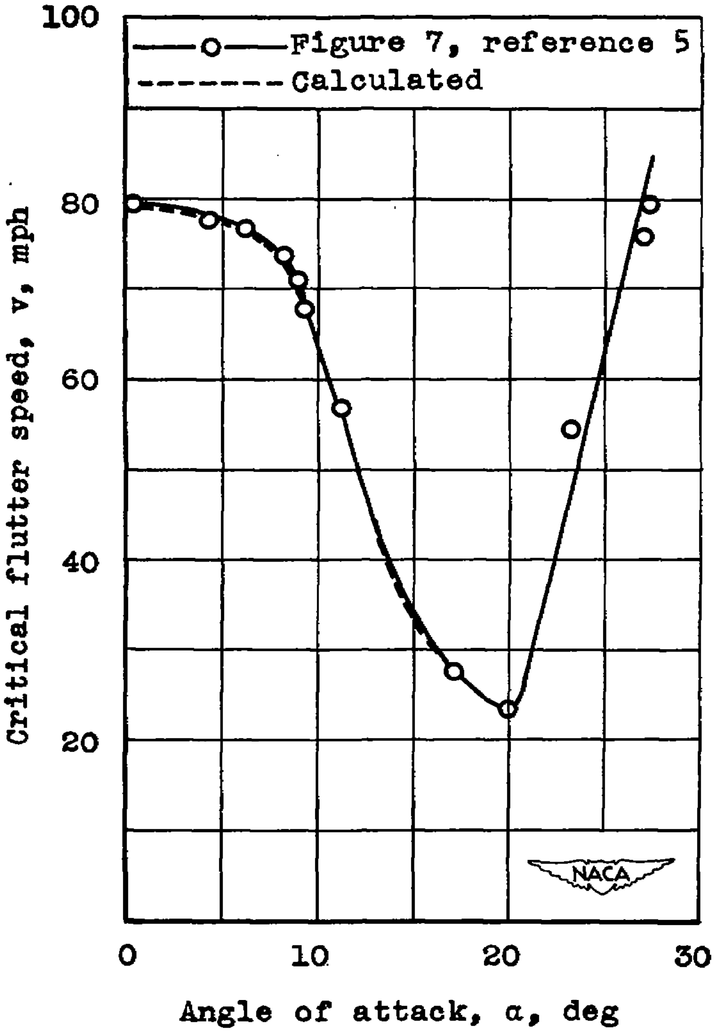

Figure 6. - Variation of critical flutter speed with angle of attack.

914

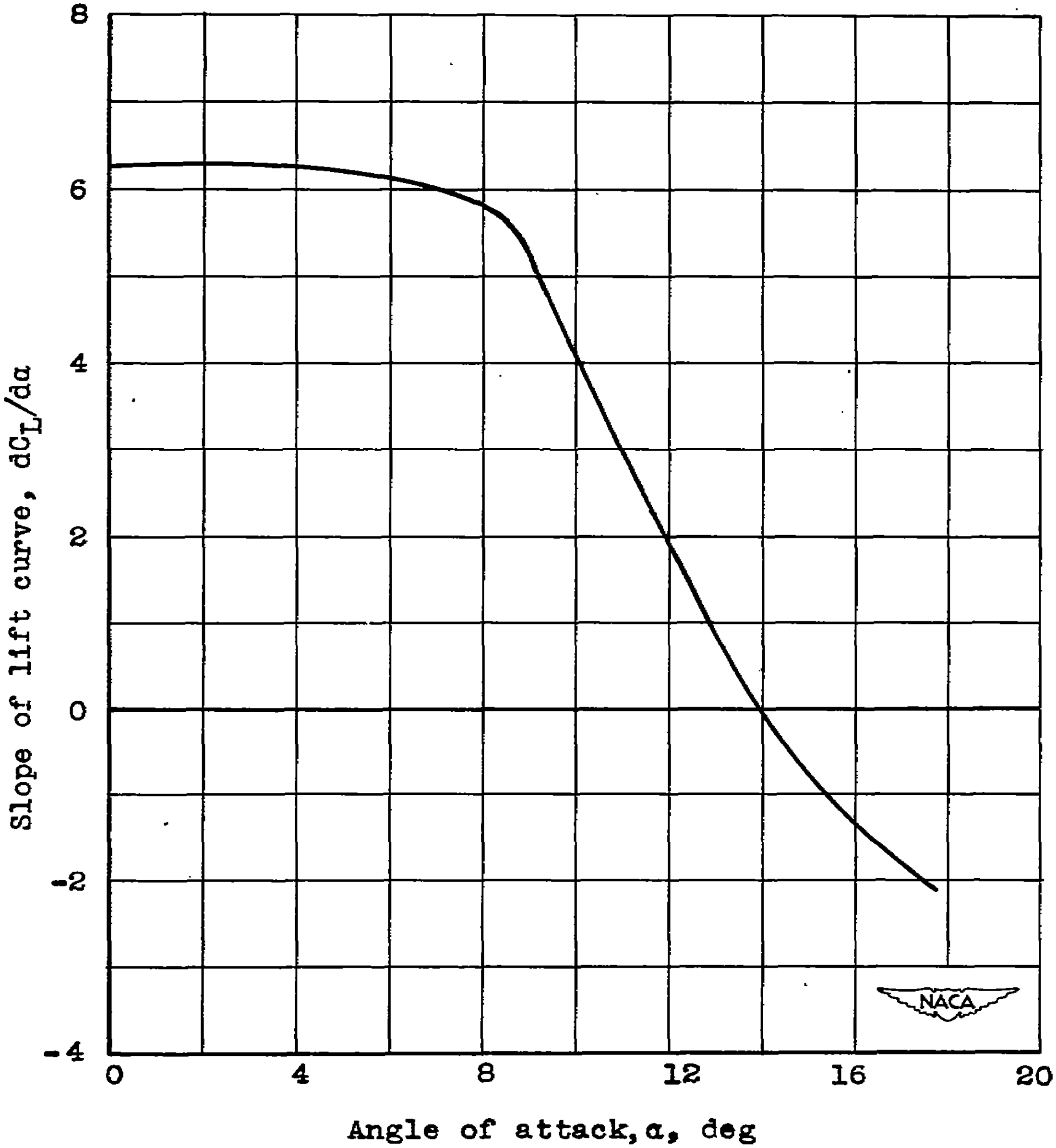

Figure 7. - Variation of slope of lift curve with angle of attack. (Based on fig. 8, reference 5.)

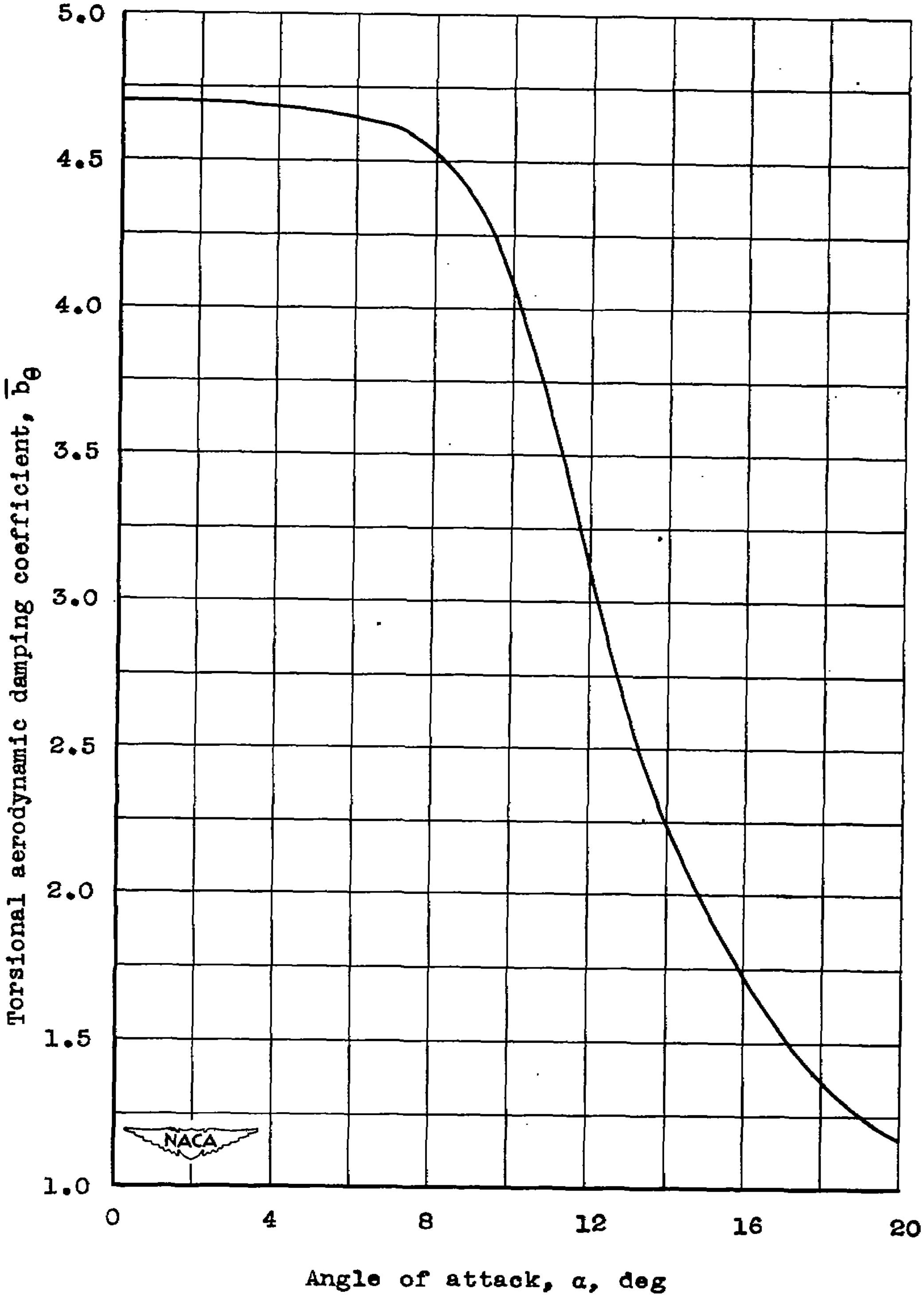

Figure 8. - Variation of calculated torsional aerodynamic damping coefficient with angle of attack.